

Research Article

# Photosensitive Semiconductor GaAs Based High Sensitivity Terahertz Metamaterial Biosensor for Multi-Virus Detection

Ashwani Kumar\* , Vikas Yadav 

Department of Electronic Science, University of Delhi South Campus, New Delhi, India

## Abstract

In the present paper, a study and design is presented of a High Sensitivity Terahertz Metamaterial Biosensor for the detection of multiple viruses using the photosensitive semiconductor GaAs. The biosensor comprises a layered structure: a semiconductor GaAs layer at the top, a gold (Au) conductor layer in the middle, and a polyimide substrate at the base. Numerical experimentation in CST Microwave Studio validates the biosensor's efficacy against several dangerous viruses including Early Cancer, Malaria, Dengue, HIV, among others. It exhibits an average sensitivity of 1.673 THz/RIU, a quality factor of 510, and a high Figure of Merit (FOM) of 418.3 RIU-1. Notably, the biosensor demonstrates polarization insensitivity, accommodating both Transverse Electric (TE) and Transverse Magnetic (TM) polarization states. Moreover, its performance is tunable by varying the conductivity via photo-excitation-induced free carriers in GaAs. This versatile biosensor holds significant promise in terahertz technology, particularly within the medical field, for the sensitive detection of multiple viruses. Its unique design and high sensitivity make it a valuable tool for early disease detection and monitoring. Moving forward, further research and development could enhance its applicability and refine its performance characteristics, paving the way for advancements in the rapid and accurate diagnosis of various infectious diseases.

## Keywords

Absorber, Biosensor, Gallium Arsenide (GaAs), Metamaterial, Terahertz

## 1. Introduction

The terahertz frequency lies between the visible and microwave frequency ranges. Recently, researchers worldwide have recognized the potential of terahertz (THz) frequencies for numerous applications in telecommunications [1], imaging [2], and sensing [3-7], offering advantages over conventional technologies. Metamaterials with unique properties, such as a negative refractive index (RI) and negative dielectric constant, are used to control and manipulate terahertz elec-

tromagnetic waves. THz waves have extremely low photon energies—one THz wave corresponds to approximately 4.14 meV, resulting in minimal radiation damage and no ionization of biomolecules [8, 9]. Terahertz Time-Domain Spectroscopy (THz-TDS) technology shows great promise in detecting biomedical and toxic chemicals [10]. However, the detection sensitivity of THz-TDS can sometimes be inadequate for specific substances, such as early-stage cancer detection and

\*Corresponding author: [ashwanikumar7@yahoo.com](mailto:ashwanikumar7@yahoo.com) (Ashwani Kumar)

Received: 17 January 2025; Accepted: 27 January 2025; Published: 17 February 2025



Copyright: © The Author(s), 2025. Published by Science Publishing Group. This is an **Open Access** article, distributed under the terms of the Creative Commons Attribution 4.0 License (<http://creativecommons.org/licenses/by/4.0/>), which permits unrestricted use, distribution and reproduction in any medium, provided the original work is properly cited.

multi-virus detection. As a result, there has been significant interest in developing terahertz absorbers for sensing applications in recent years [3-7]. Ongoing efforts are focused on designing high-sensitivity THz absorbers for biosensing, with the first experimental realization of a perfect metamaterial absorber in the microwave frequency range [11]. Through their distinct spectral responses and biomolecular interactions, recent investigations have shown the promise of THz-based sensors for the detection of a variety of viruses, including HIV, SARS-CoV-2, and influenza [12, 13]. These sensors' increased sensitivity allows for the detection of low virus quantities in complicated samples by combining cutting-edge THz technology with nanomaterials like carbon nanotubes or gold nanoparticles [14]. Additionally, the creation of multiplexed THz biosensors has enormous potential for the simultaneous detection of several viruses in a single test, which would make them indispensable for pandemic response and worldwide health monitoring [15].

In recent years, various THz biosensor designs incorporating innovative materials such as graphene [3], gold [4], InSb [5], 3D metals [6], and GaAs [7] have been proposed for diagnostics, medicine, and biomolecular analysis. However, graphene-based sensors are complex to design and tune, with limited maximum absorption efficiency. Similarly, gold, InSb, and 3D metal-based absorbers, while promising, suffer from low-quality factors and sensitivity. Improving the quality factor and sensitivity remains a significant challenge.

In this work, we present a semiconductor GaAs-based photosensitive biosensor for multi-virus detection with an average sensitivity of 1.673 THz/RIU, a quality factor (Q) of 510, and a Figure of Merit (FOM) of 418.3 RIU<sup>-1</sup>. The proposed biosensor is polarization-insensitive for both TE and TM polarizations and tunable with respect to conductivity changes induced by photo-excitation-generated free carriers in GaAs. The tunability of the sensor expands its sensing bandwidth, making it suitable for various biomedical sensing applications, disease diagnosis, and more.

## 2. Design of GaAs Metamaterial Absorber (Biosensor)

The suggested high-sensitivity metamaterial biosensor based on the photosensitive semiconductor GaAs is shown schematically in Figure 1. The biosensor is composed of three layers: the top layer is composed of GaAs semiconductor with a thickness of  $t=10\ \mu\text{m}$ , the intermediate gold layer is  $0.2\ \mu\text{m}$  thick, and the bottom substrate polyimide layer is  $h=50\ \mu\text{m}$ . The conductivity of gold is  $3.56 \times 10^7\ \text{S/m}$ , while the relative dielectric constant of the top layer GaAs is  $\epsilon_r = 12.9 + 0.0774i$ . The dielectric constant of the bottom polyimide substrate is  $\epsilon_r = 3.5$ .  $P=140 \times 140\ \mu\text{m}$  is the unit cell's size. With a thickness of  $t = 10\ \mu\text{m}$ , the outer circular ring has a radius of  $R = 48.5\ \mu\text{m}$  and an inner radius of  $R_1 = 40\ \mu\text{m}$ . Figure 1 displays the unit cell's optimal dimensions

as follows: The thickness of the polyimide substrate is  $h=50\ \mu\text{m}$ , and the period is indicated by  $P = 140\ \mu\text{m}$ . Figure 2 illustrates the functionality of the suggested GaAs-based terahertz biosensor in the absence of an analyte or virus cells. At a center frequency of 2.04 THz, it exhibits 100% absorption with a quality factor (Q) of 510.

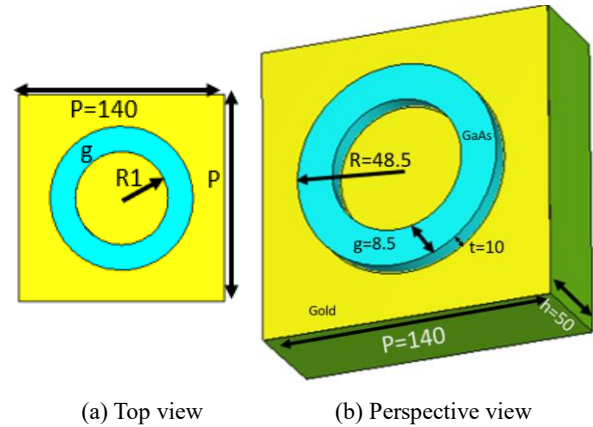


Figure 1. Schematic diagram of the proposed GaAs biosensor.

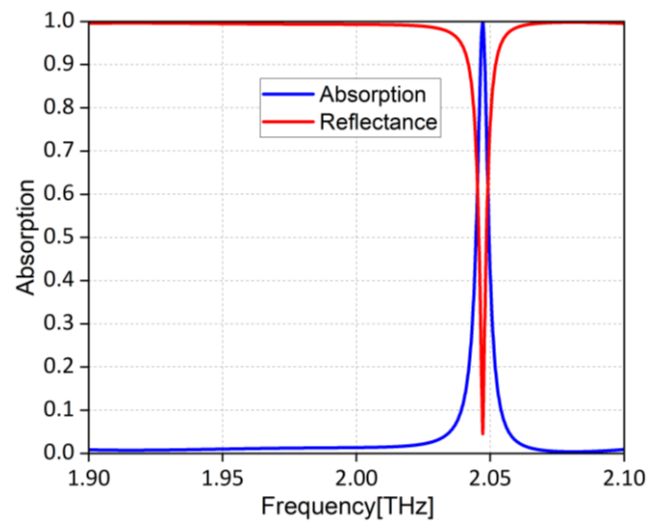


Figure 2. Performance of proposed GaAs Biosensor.

The suggested biosensor was designed using CST Microwave Studio. The periodic boundary condition was set in the X and Y directions, and the entirely matched layer boundary condition was established in the Z direction for the CST simulation. The simulation of the absorber ranges from 1.9 to 2.10. The reflectivity R of the metamaterial for the normal incidence of the THz wave is determined by the Fresnel formula.

$$R = \left| \frac{Z-Z_0}{Z+Z_0} \right|^2 = \left| \frac{\sqrt{\mu_r} - \sqrt{\epsilon_r}}{\sqrt{\mu_r} + \sqrt{\epsilon_r}} \right|^2 \quad (1)$$

Where  $Z$  is the impedance of the material, which is  $\left(\sqrt{\frac{\mu}{\epsilon}}\right)$  and  $Z_0$  is the impedance of free space, which is  $\left(\sqrt{\frac{\mu_0}{\epsilon_0}}\right)$ . The  $\epsilon_r$  and  $\mu_r$  are the relative permittivity and permeability of the material, while  $\mu_0 = 4\pi \times 10^{-7}$  H/m and  $\epsilon_0 = 8.85 \times 10^{-12}$  F/m are the free space relative permittivity and permeability, respectively. Absorption is given as  $A=1-R-T$ , where  $R$  is reflectance, and  $T$  is transmittance. Since transmittance is considered zero because of the pure conducting backside of the GaAs, hence absorption can be obtained using equation (2).

$$A = 1 - R = 1 - \left| \frac{Z-Z_0}{Z+Z_0} \right|^2 = 1 - \left| \frac{\sqrt{\mu_r} - \sqrt{\epsilon_r}}{\sqrt{\mu_r} + \sqrt{\epsilon_r}} \right|^2 \quad (2)$$

The impedance matching theory states that the effective permittivity and permeability of metamaterials can be adjusted to match the absorber's impedance with free space, or  $Z=Z_0$ . This requires that the material's permeability and permittivity be equal.

### 3. Absorber as Biosensor for Multi-Virus Detection

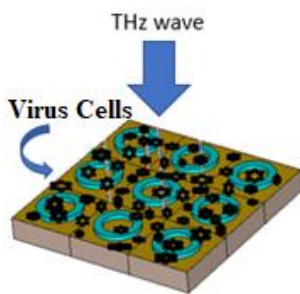


Figure 3. THz metamaterial biosensor with virus cells.

This section demonstrates how the absorber that was designed in part II can be used as a biosensor to identify cancer and multi-virus in its early stages. As illustrated in Figure 3, the Multi-Vrus and cancer cells or analytes have been positioned above the THz metamaterial absorber.

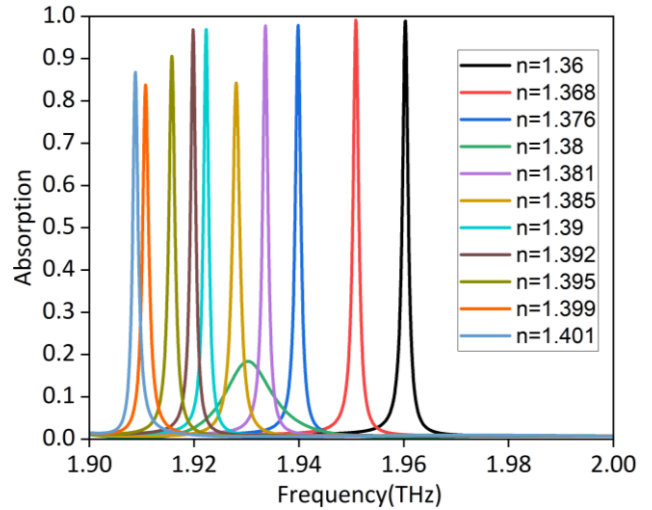


Figure 4. Absorbance with different refractive indexes of various cancer cells.

For instance, in the first case, we are using the refractive index of the cancer cells on the proposed metamaterial GaAs absorber. The absorbance of the biosensor with the different refractive index (RI) for various cancer cells and with normal cells is plotted in Figure 4. When the refractive index (RI) of cancer cells varies, the resonance frequency falls as the RI increases. Figure 4 illustrates the biosensor's performance using a range of cancer cells with variable refractive indices (RIs).

Table 1. Resonance frequencies with different cancer cells.

S. N.	Cell Name	State	Refractive Index (n)	Resonance Frequency (GHz)	Sensitivity (GHz/RIU)
1	air	air	1	2046	1653.4
2	Besal cell	Normal	1.36	1962	1650.0
		Cancer	1.38	1929	
3	Breast Cell	Normal	1.385	1931	1571.4
		Cancer	1.399	1909	
4	Cervical Cell	Normal	1.368	1956	1583.3
		Cancer	1.392	1918	
5	Jurkat	Normal	1.376	1944	1571.4
		Cancer	1.39	1922	

S. N.	Cell Name	State	Refractive Index (n)	Resonance Frequency (GHz)	Sensitivity (GHz/RIU)
6	MCF-7	Normal	1.36	1962	1585.4
		Cancer	1.401	1908	
7	PC12	Normal	1.381	1933	1642.9
		Cancer	1.395	1915	

**Table 2.** Resonance frequencies with different Viruses.

S. N.	Virus	Refractive Index (n)	Resonance Frequency (GHz)	Sensitivity (GHz/RIU)
1.	air	1.0	2046	1653.4
2.	Malaria (n1)	1.373	1945	270.7
3.	Malaria (n2)	1.383	1932	297.6
4.	Dengue	1.4	1914	330
5.	HSV	1.41	1899	358.5
6.	Influenza A	1.48	1851	406.2
7.	HIV	1.5	2187	282
8.	Corona	1.53	2150	196.2

Table 1 and Table 2 compare the resonance frequency with different cancer cells and Multi-Virus (Malaria, Dengue, and HIV etc.) and tabulate the sensitivity for different refractive indexes. The sensitivity can be defined as  $S_f = \frac{\Delta f}{\Delta n}$  GHz/RIU, Quality factor (Q) can be defined as  $Q = \frac{f}{FWHM}$ , and Figure of merit (FOM) can be defined as  $FOM = \frac{S_f}{FWHM}$ . Where  $\Delta f$  is the change in frequency,  $\Delta n$  is the change in the refractive index, and FWHM is the full-width half maximum of the resonance absorption. Our proposed biosensor has an average sensitivity is 1650 GHz/RIU, while the average quality factor Q is 510 and a Figure of merit (FOM) of 418.3 RIU<sup>-1</sup>. Since the GaAs-based biosensor structure is symmetric, the performance with a normal incident of transverse electric (TE) waves and transverse magnetic wave TM, the absorbance is the same. Hence, we can say that the proposed biosensor is polarization-insensitive. The performance linearity of the proposed biosensor for Multi-Virus and cancer early detection is shown in Tables 1 and 2, with the refractive index starting from  $n = 1.36$  to  $1.401$  and multi-virus from  $n=1.373$  to  $1.53$ . Cancer cells and normal cells are tabulated in Table 1, while Table 2 is for multi-virus.

Figure 5 shows the resonance frequency dependence on the cancer cells' refractive index (RI), and variation is plotted in Figure 5, which shows that the proposed biosensor has a linear response and can be a linear curve fitting done in equation (3).

$$freq = 1.2802n + 3.7018 \quad (3)$$

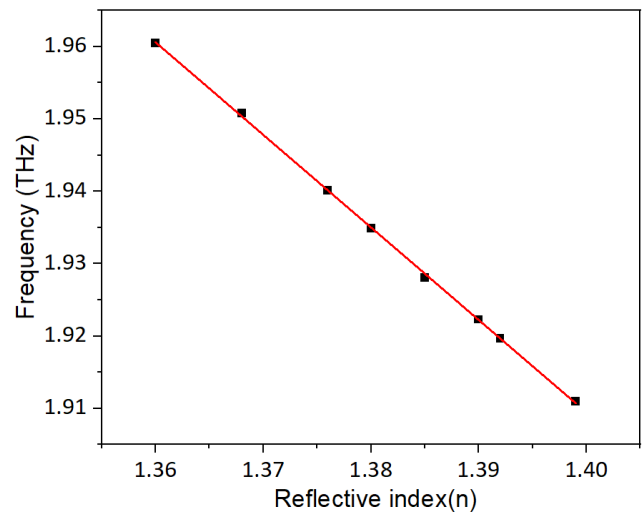


**Figure 5.** The resonance frequency dependence on the cancer cell refractive index (RI).

Where  $n$  is the cancer cell refractive index (RI), and frequency is the corresponding resonance frequency. The proposed biosensor operation is based on the refractive index (RI) of various virus cells, denoted as  $n$ , and the corresponding

resonance frequency. This design enables the detection of cancer cells at very early stages, boasting an average sensitivity of 1650 GHz/RIU. Moreover, the biosensor is versatile, demonstrating the capability in detecting multiple viruses. Comparative analysis against recently published research in similar cancer cells RI designs highlights the superior performance of our GaAs-based metamaterial biosensor. Evaluation from Table 3 underscores that our biosensor excels in

sensitivity, quality factor, and Figure of Merit (FOM) compared to previous studies. These metrics substantiate the advanced performance of our proposed biosensor. Numerical experimentation confirms the efficacy of our biosensor for critical applications in early cancer detection. The design is straightforward yet highly effective, surpassing the benchmarks set by recent studies in the field.

**Table 3.** Comparison of our absorber with the recent work.

Ref	Materials	Q factor	FoM (RIU <sup>-1</sup> )	Sensitivity (THz/RIU)	Tunability
[3]	Graphene	---	24	1.775	Yes
[4]	Gold	57	11.5	0.281	No
[5]	InSb	53	---	1.043	No
[6]	3D metal	72	---	0.832	No
[7]	GaAs	444	392	1.762	Yes
Our	GaAs	510	418.3	1.673	Yes

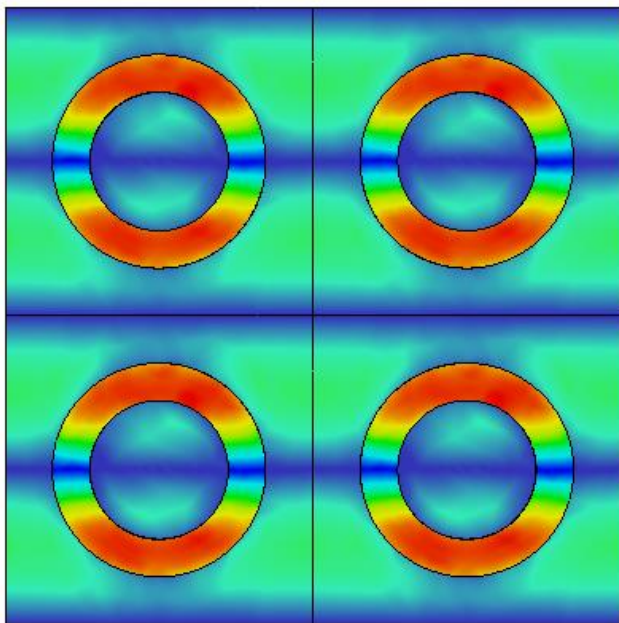


**Figure 6.** Electric field distribution on the GaAs biosensor at 1.9THz.

Figure 6 depicts the distribution of the electric field across the biosensor at a frequency of 1.9 THz. The visualization reveals that the regions of highest electric field intensity concentrate predominantly in the upper and lower halves of the circular GaAs ring. This pattern indicates that the designed biosensor efficiently interacts with electromagnetic waves in the terahertz (THz) range. The significant concentration of electric field suggests that the biosensor can effectively detect and interact with external THz radiation. This characteristic is crucial for its intended application in sensing biological viruses, particularly viruses of cancer cells. Due to the heightened interaction with THz waves, the biosensor exhibits high sensitivity. This sensitivity enhances its capability to detect minute quantities of biomolecules or cells, thereby enabling early-stage detection of multiple viruses and cancer.

The tunability in the proposed biosensor can be realized by generating the free charge carriers with the photon excitation in photosensitive semiconductor GaAs. This can be understood by looking carefully at the frequency response with different conductivity variations. As the conductivity changes from  $\sigma=0$  S/m to  $7 \times 10^5$  S/m, the resonance frequency of the proposed biosensor varied. Hence, we can say that by illuminating photosensitive semiconductor GaAs with photons, the conductivity can be changed, and the biosensor can be tuned, as shown in Figure 7.

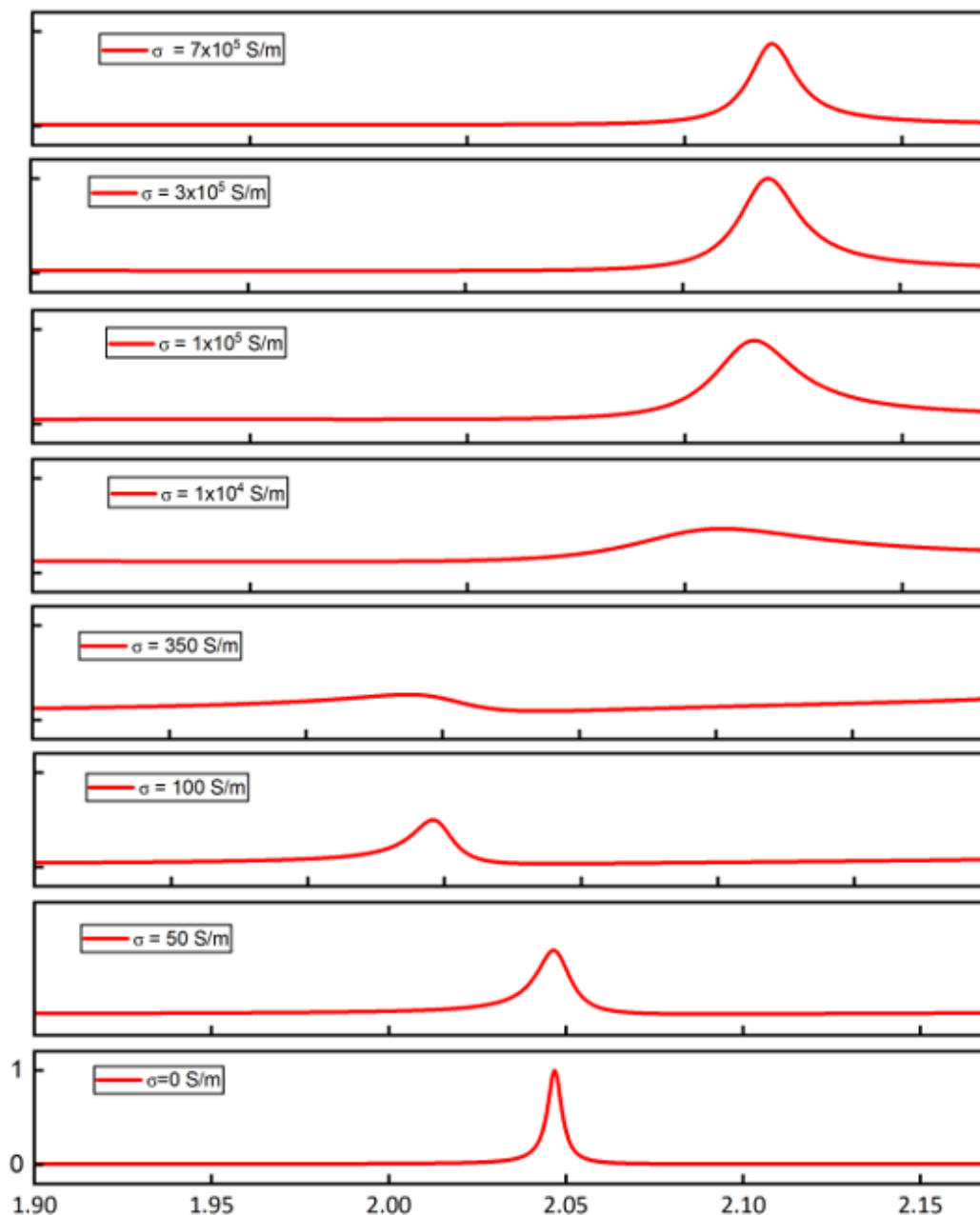


**Figure 7.** Variation in resonance frequency of the absorption of the proposed semiconductor GaAs biosensor for different conductivity.

## 4. Conclusion

This paper presents a photosensitive semiconductor GaAs-based metamaterial biosensor for the early detection of multiple viruses and cancer. The biosensor exhibits an average sensitivity of 1.65 THz/RIU, a quality factor of 510, and a Figure of Merit (FOM) of 418.3 RIU<sup>-1</sup>. It is polarization-insensitive for both TE and TM polarizations and can be tuned through changes in conductivity induced by photo-excitation, which generates free carriers in GaAs. The proposed biosensor holds promise for applications in terahertz (THz) technology, particularly in the medical field for early cancer detection.

## Abbreviations

GaAs	Gallium Arsenide
FOM	Figure of Merit
THz	Terahertz
FWHM	Full-Width Half Maximum
RI	Refractive Index
THz-TDS	Terahertz Time-Domain Spectroscopy
TE	Transverse Electric
TM	Transverse Magnetic
Q	Quality Factor

## Author Contributions

**Ashwani Kumar:** Conceptualization, Data curation, Writing – review & editing

**Vikas Yadav:** Data curation, Investigation

## Funding

This work is supported by Faculty Research Programme Grant – IoE, University of Delhi (Grant No. Ref. No./IoE/2024-25/12/FRP)

## Conflicts of Interest

The authors declare no conflicts of interest.

## References

- [1] C. Huang, Z. Yang, G. C. Alexandropoulos, K. Xiong, L. Wei, C. Yuen Z. Zhang, M. Debbah, Multi-hop RIS-empowered terahertz communications: a DRL-based hybrid beamforming design, *IEEE J. Sel. Area. Commun.* 39 (2021): 1663–1677, <https://doi.org/10.1109/JSAC.2021.3071836>
- [2] H. Guerboukha, K. Nallappan, M. Skorobogatiy, “Toward real-time terahertz imaging”, *Advances in Optics and Photonics*, 10 (2018) 843, <https://doi.org/10.1364/AOP.10.000843>
- [3] Zhihui He, Lingqiao Li, Huqiang Ma, Lihui Pu, Hui Xu, Zao Yi, Xinliang Cao, Wei Cui, “Graphene-based metasurface sensing applications in terahertz band”, *Results in Physics*, Vol. 21, 2021, 103795, <https://doi.org/10.1016/j.rinp.2020.103795>
- [4] L. Zhu et al., "Dual-band electromagnetically induced transparency (EIT) terahertz metamaterial sensor," *Opt. Material Exp.*, vol. 11, no. 7, pp. 2109–2121, Jul. 2021, <https://doi.org/10.1364/OME.425126>
- [5] Y. Cheng, Z. Li, and Z. Cheng, "Terahertz perfect absorber based on InSb metasurface for both temperature and refractive index sensing," *Optical Material.*, vol. 117, Jul. 2021, Art. no. 111129, <https://doi.org/10.1016/j.optmat.2021.111129>
- [6] J. P. Yang, H. Deng, Z. G. Xiong, and L. P. Shang, "Terahertz sensor based on a three-dimensional double I-type metamaterial integrated microfluidic channel," *Appl. Opt.*, vol. 60, no. 13, pp. 3816–3822, May 2021, <https://doi.org/10.1364/AO.421910>
- [7] Jingwen Wu, Tingting Yuan, Jianjun Liu, Jianyuan Qin, Zhi Hong, Jiusheng Li, and Yong Du, "Terahertz Metamaterial Sensor With Ultra-High Sensitivity and Tunability Based on Photosensitive Semiconductor GaAs", *IEEE Sensors Journal*, Vol. 22, No. 16, 15 August 2022, <https://doi.org/10.1109/JSEN.2022.3190414>
- [8] C. Jansen et al., "Terahertz imaging: Applications and perspectives," *Appl. Opt.*, vol. 49, no. 19, pp. 48–57, 2010.
- [9] X. Yang et al., "Biomedical applications of terahertz spectroscopy and imaging," *Trends Biotechnol.*, vol. 34, no. 10, pp. 810–824, Oct. 2016, <https://doi.org/10.1016/j.tibtech.2016.04.008>
- [10] S. Wang et al., "Terahertz biosensing based on a polarization-insensitive metamaterial," *IEEE Photon. Technol. Lett.*, vol. 28, no. 9, pp. 986–989, May 1, 2016, <https://doi.org/10.1109/LPT.2016.2522473>
- [11] N. I. Landy, S. Sajuyigbe, J. J. Mock, D. R. Smith, W. J. Padilla, A perfect metamaterial absorber, *Phys. Rev. Lett.* 100 (2008), 207402, <https://doi.org/10.1103/PhysRevLett.100.207402>
- [12] Naznin Akter, Muhammad Mahmudul Hasan, and Nezhil Pala, "A Review of THz Technologies for Rapid Sensing and Detection of Viruses including SARS-CoV-2", *Biosensors*, 2021, 11(10), 349; <https://doi.org/10.3390/bios11100349>
- [13] W. Bian, S. Li, T. Zhang, S. Zhang, Y. Chen and Z. Li, "Rapid Detection of Four Foodborne Pathogens Based on Terahertz Time Domain Spectroscopy," *2024 IEEE International Conference on Manipulation, Manufacturing and Measurement on the Nanoscale (3M-NANO)*, Zhongshan, China, 2024, pp. 549-554, <https://doi.org/10.1109/3M-NANO61605.2024.10769637>
- [14] Peng Shen, Yunyun Ji, Xinmin Yue, Yifeng Li, Mengfan Han, Yan Ma, Meng Meng, Fei Fan, Shengjiang Chang, “Ultrasensitive terahertz microfluidic biosensor integrated with tetrahedral DNA nanostructure for specific detection of live cancer cells”, *Sensors and Actuators B: Chemical*, Vol. 428, 2025, <https://doi.org/10.1016/j.snb.2025.137252>
- [15] Almeida, M. B. D., Schiavo, L., Esmanhoto, E., Lenz, C. A., Rocha, J., Loureiro, M.,... & Barros Filho, "Terahertz spectroscopy applied to diagnostics in public health: A review", *Brazilian Archives of Biology and Technology*", 64, e21200770, <https://doi.org/10.1590/1678-4324-75years-2021200770>